Nigerian Journal of Technology (NIJOTECH)
Vol. 43, No. 4, December, 2024, pp.646 - 654
www.nijotech.com

Print ISSN: 0331-8443
Electronic ISSN: 2467-8821
https://doi.org/10.4314/njt.v43i4.5

FREE VIBRATION ANALYSIS OF THIN RECTANGULAR PLATES USING PIECEWISE SHAPE FUNCTIONS IN RITZ PROCEDURE

AUTHORS:
A. Adamou[1,*]

AFFILIATIONS:
[1]Ecole Supérieure des Sciences du Numérique, Université de Dosso, Niger.

***CORRESPONDING AUTHOR:**
Email: amadamousoul@yahoo.com

ARTICLE HISTORY:
Received: 07 August, 2024.
Revised: 14 November, 2024.
Accepted: 18 November, 2024.
Published: 31 December, 2024.

KEYWORDS:
Comparison function, Free vibration, Frequency parameter, Piecewise trial function, Rectangular plate.

ARTICLE INCLUDES:
Peer review

DATA AVAILABILITY:
On request from author(s)

EDITORS:
Chidozie Charles Nnaji

FUNDING:
None

Abstract

In the present work, piecewise functions have been successfully built in the form of polynomials to be utilised in the Ritz procedure to carry out the free vibration analysis of thin rectangular plates. They were consistently constructed by considering the plate as consisting of equal strips in its two perpendicular directions, and could be generated for all the combinations of plate's classical edge supports. The procedure was performed for different combinations of simple and/or clamped plate's boundary supports, taking into account four aspect ratios (1, 1.5, 2 and 2.5), and the first six frequency parameters were retained. These frequency parameters were found to be in good concordance with the available exact and approximate solutions. For example, for a square plate with simple supports, the percentage differences, comparatively to the exact Navier solutions, ranged from - 0.007% (for the fundamental mode) to - 1.534% (for the sixth mode). Similar trends were obtained for the other aspect ratios and sets of boundary conditions considered. For all the boundary conditions studied, it was observed an increase in value of the frequency parameters with that of the plates' side ratios. In addition, for each of the modes considered, it was found out that the computed frequency parameters increased consistently when the number of clamped edges increased in the set of the plate's boundary conditions. The practical consequence is that thin rectangular plates with clamped edges may witness resonance when the forcing frequencies are high, while they can resist the low and medium ones.

1.0 INTRODUCTION

Thin plates are common structures found in different fields of engineering due to the fact that they are economical beside their efficient load-carrying capacity [1], [2], [3]. They are often subjected to dynamic loads during their life span. Thus, their design requires the knowledge of their behaviour under dynamic excitation in order to avoid their failure which may occur under resonance. Hence the dynamic analysis of rectangular becomes interestingly important.

Besides the exact methods which are applicable to only few cases of rectangular plates [4], researchers and practitioners resort to approximates solutions such as the Ritz method. Ritz method strongly relies on the selection of the right trial functions making up the shape function used in the procedure. In most cases the trial functions are chosen intuitively by the analyst, instead of being generated systematically. However, researchers [5], [6], agree that the chosen functions

HOW TO CITE:
Adamou, A. "Free Vibration Analysis of Thin Rectangular Plates using Piecewise Shape Functions in Ritz Procedure", *Nigerian Journal of Technology*, 2024; 43(4), pp. 646 – 654; https://doi.org/10.4314/njt.v43i4.5

© 2024 by the author(s). This article is open access under the CC BY-NC-ND license

must satisfy at least the geometric boundary conditions (such functions are said to be admissible) and must be independent linearly for accurate and convergent eigenvalues to be obtained. When they are selected such that, they satisfy all the boundary conditions (in which case they are called comparison functions), the accuracy of the solutions might be significantly improved. Polynomial trial functions are the most frequently used, even though it is not unusual to encounter transcendental shape functions [5]. They are known to allow straightforward algebraic manipulation, and to deliver accurate practical results in Ritz procedure.

The Ritz procedure was successfully utilised by Adah, et al [7] to compute the resonating frequency of a vibrating plate of various aspect ratios and boundary conditions. The polynomial shape functions they used contained only one term in the form of a product of two four-degree polynomials in the two perpendicular directions of the plate. Thus, the computer program they developed gave only the fundamental natural frequencies. Similar shape functions were used by Asomugha, et al [8] in Ritz procedure to compute the fundamental resonating frequency parameters for a rectangular plate that has two opposite simple edge supports whereas the other two are fixed (CSCS), and one presenting three simply supported edges and one edge clamped (CSSS), under various aspect ratios.

The present study applies the Ritz method to the free vibration analysis of thin rectangular plates presenting different side ratios and combining simple and/or fixed boundaries. Piecewise polynomial trial functions are built by considering real deformation patterns of the plate structures, for the purpose of determining frequency parameters of various thin rectangular plates using the Ritz procedure. Mathematica software is used for the mathematical manipulation involved, hence reducing the inherent computation errors.

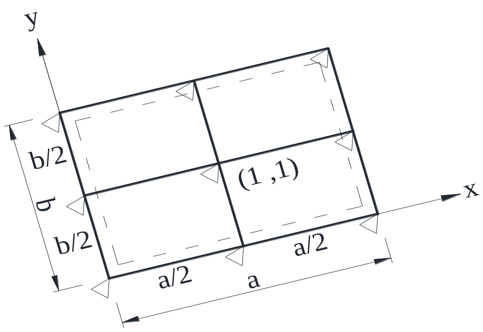

Figure 1: Simply supported rectangular plate split into two equal strips in the directions of x and y

2.0 METHODOLOGY

2.1 Derivation of the Piecewise Polynomial Trial Functions

Consider an all-round simply supported thin rectangular plate. The plate is split into finite and equal numbers of strips in its two perpendicular directions represented by x and y. Simple supports are introduced at the nodes determined by the axes of the perpendicular strips. The supports at the edges are also simple since the plate is considered to be simply supported (See Figure 1).

The shape function is sought in the form:

$$W(x,y) = \sum_{i=1}^{n}\sum_{j=1}^{m} C_{ij}X_i(x)Y_j(y) \quad (1)$$

Where, C_{ij} is the nodal displacement of node (i,j), $X_i(x)$ and $Y_j(y)$ are elastic unit curves in x and y directions respectively due to unit deflection induced at node (i,j).

In order to determine $X_i(x)$ and $Y_j(y)$, a unit deflection is induced at node $(i,j)[ie: C_{ij} = 1]$. On the assumption that the strips (in x and y directions) whose axes intersect at the node (i, j) behave as beams, the bending moments M_i and M_j in the directions of x and y respectively due to the unit deflection at the node (i, j) are first plotted using, for example, the displacement method (see Figure 2); then their expressions are derived from the plots. The expressions of M_i and M_j will be piecewise linear polynomials of x and y respectively. Furthermore, it is well documented from strength of materials that:

$$M_i(x) = -\frac{d^2X_i(x)}{dx^2}EI_i \quad (2)$$

and

$$M_j(x) = -\frac{d^2Y_j(y)}{dy^2}EI_j \quad (3)$$

Where, E stands for the Young modulus of the material of the plate, and I_i and I_j are the moments of inertia of the strips in x and y directions respectively.

Double integration of the Equation (2) and Equation (3) yields the expressions of $X_i(x)$ and $X_j(y)$ upon application of the corresponding boundary conditions.

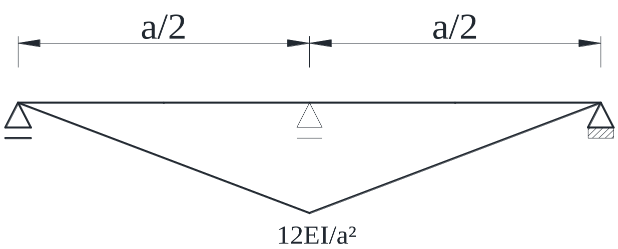

Figure 2: Strip bending moment diagram in x direction induced by a unit deflection applied at node (1, 1) when the simply supported plate is divided into two equal strips

© 2024 by the author(s). Licensee NIJOTECH.
This article is open access under the CC BY-NC-ND license.
http://creativecommons.org/licenses/by-nc-nd/4.0/

As an illustration, if we divide the plate into two strips in x and y directions, only one intermediary support will be introduced while the other supports will be on the plate edges (see Figure 1). Thus, we will have only one node (1, 1). The expressions of associated bending moments will be (see Figure 2):

$$M_1(x) = \begin{cases} \frac{24EI_1}{a^3}x & if\ 0 \le x \le \frac{a}{2} \\ -\frac{24\,EI_1}{a^3}x + \frac{24\,EI_1}{a^2} & if \frac{a}{2} \le x \le a \end{cases} \quad (4)$$

and

$$M_1(y) = \begin{cases} \frac{24EI_1}{b^3}y & if\ 0 \le y \le \frac{b}{2} \\ -\frac{24\,EI_1}{b^3}y + \frac{24\,EI_1}{b^2} & if \frac{b}{2} \le y \le b \end{cases} \quad (5)$$

Where, a and b are the dimensions of the plate corresponding to the directions of x and y respectively.

Making use of Equation (4) and Equation (5) in Equation (2) and Equation (3) respectively, carrying out successive integration and considering the boundary conditions, the expressions $X_1(x)$ and $Y_j(y)$ are obtained as follows:

$$X_1(x) = \begin{cases} -\frac{4}{a^3}x^3 + \frac{3}{a}x & if\ 0 \le x \le a/2 \\ \frac{4}{a^3}x^3 - \frac{12}{a^2}x^2 + \frac{9}{a}x - 1 & if\ a/2 \le x \le a \end{cases} \quad (6)$$

and

$$Y_1(y) = \begin{cases} -\frac{4}{b^3}y^3 + \frac{3}{b}y & if\ 0 \le y \le b/2 \\ \frac{4}{b^3}y^3 - \frac{12}{b^2}y^2 + \frac{9}{b}y - 1 & if\ b/2 \le y \le b \end{cases} \quad (7)$$

For convenience, the expressions $X_1(x)$ and $Y_j(y)$ are made dimensionless by letting $\xi = x/a$ and $\eta = y/b$:

$$X_1(\xi) = \begin{cases} -4\xi^3 + 3\xi & if\ 0 \le \xi \le \frac{1}{2} \\ 4\xi^3 - 12\xi^2 + 9\xi - 1 & if \frac{1}{2} \le \xi \le 1 \end{cases} \quad (8)$$

and

$$Y_1(\eta) = \begin{cases} -4\eta^3 + 3\eta & if\ 0 \le \eta \le \frac{1}{2} \\ 4\eta^3 - 12\eta^2 + 9\eta - 1 & if \frac{1}{2} \le \eta \le 1 \end{cases} \quad (9)$$

It is important to note that the expressions $X_1(x)$ and $Y_j(y)$ as expressed in Equation (8) and Equation (9) should then be substituted into Equation (1) for implementation of the Ritz method. In that case the Ritz method reduces to that of Raleigh whereby the shape function is made of only one term.

Using a similar procedure, the following trial functions will be derived for the cases below:

❖ Consideration of three strips in the directions of x and y respectively:

In the direction of x

$$X_1(\xi) = \begin{cases} -\frac{81}{5}\xi^3 + \frac{24}{5}\xi & if\ 0 \le \xi \le \frac{1}{3} \\ 27\xi^3 - \frac{216}{5}\xi^2 + \frac{96}{5}\xi - \frac{8}{5} & if \frac{1}{3} \le \xi \le \frac{2}{3} \\ -\frac{54}{5}\xi^3 + \frac{162}{5}\xi^2 - \frac{156}{5}\xi + \frac{48}{5} & if \frac{2}{3} \le \xi \le 1 \end{cases} \quad (10)$$

$$X_2(\xi) = \begin{cases} \frac{54}{5}\xi^3 - \frac{6}{5}\xi & if\ 0 \le \xi \le \frac{1}{3} \\ -27\xi^3 + \frac{189}{5}\xi^2 - \frac{69}{5}\xi + \frac{7}{5} & if \frac{1}{3} \le \xi \le \frac{2}{3} \\ \frac{81}{5}\xi^3 - \frac{243}{5}\xi^2 + \frac{219}{5}\xi - \frac{57}{5} & if \frac{2}{3} \le \xi \le 1 \end{cases} \quad (11)$$

In the direction of y

$$Y_1(\eta) = \begin{cases} -\frac{81}{5}\eta^3 + \frac{24}{5}\eta & if\ 0 \le \eta \le \frac{1}{3} \\ 27\eta^3 - \frac{216}{5}\eta^2 + \frac{96}{5}\eta - \frac{8}{5} & if \frac{1}{3} \le \eta \le \frac{2}{3} \\ -\frac{54}{5}\eta^3 + \frac{162}{5}\eta^2 - \frac{156}{5}\eta + \frac{48}{5} & if \frac{2}{3} \le \eta \le 1 \end{cases} \quad (12)$$

$$Y_2(\eta) = \begin{cases} \frac{54}{5}\eta^3 - \frac{6}{5}\eta & if\ 0 \le \eta \le \frac{1}{3} \\ -27\eta^3 + \frac{189}{5}\eta^2 - \frac{69}{5}\eta + \frac{7}{5} & if \frac{1}{3} \le \eta \le \frac{2}{3} \\ \frac{81}{5}\eta^3 - \frac{243}{5}\eta^2 + \frac{219}{5}\eta - \frac{57}{5} & if \frac{2}{3} \le \eta \le 1 \end{cases} \quad (13)$$

❖ Consideration of four strips in the directions of x and y respectively:

In the direction of x

$$X_1(\xi) = \begin{cases} -\frac{272}{7}\xi^3 + \frac{45}{7}\xi & if\ 0 \le \xi \le \frac{1}{4} \\ \frac{464}{7}\xi^3 - \frac{552}{7}\xi^2 + \frac{183}{7}\xi - \frac{23}{14} & if\ \frac{1}{4} \le \xi \le \frac{1}{2} \\ -\frac{240}{7}\xi^3 + 72\xi^2 - \frac{345}{7}\xi + \frac{153}{14} & if\ \frac{1}{2} \le \xi \le \frac{3}{4} \\ \frac{48}{7}\xi^3 - \frac{144}{7}\xi^2 + \frac{141}{7}\xi - \frac{45}{7} & if\ \frac{3}{4} \le \xi \le 1 \end{cases} \quad (14)$$

$$X_2(\xi) = \begin{cases} \frac{192}{7}\xi^3 - \frac{12}{7}\xi & if\ 0 \le \xi \le \frac{1}{4} \\ -\frac{512}{7}\xi^3 + \frac{528}{7}\xi^2 - \frac{144}{7}\xi + \frac{11}{7} & if\ \frac{1}{4} \le \xi \le \frac{1}{2} \\ \frac{512}{7}\xi^3 - 144\xi^2 + \frac{624}{7}\xi - \frac{117}{7} & if\ \frac{1}{2} \le \xi \le \frac{3}{4} \\ -\frac{192}{7}\xi^3 + \frac{576}{7}\xi^2 - \frac{564}{7}\xi + \frac{180}{7} & if\ \frac{3}{4} \le \xi \le 1 \end{cases} \quad (15)$$

$$X_3(\xi) = \begin{cases} -\frac{48}{7}\xi^3 + \frac{3}{7}\xi & if\ 0 \le \xi \le \frac{1}{4} \\ \frac{240}{7}\xi^3 - \frac{216}{7}\xi^2 + \frac{57}{7}\xi - \frac{9}{14} & if\ \frac{1}{4} \le \xi \le \frac{1}{2} \\ -\frac{464}{7}\xi^3 + 120\xi^2 - \frac{471}{7}\xi + \frac{167}{14} & if\ \frac{1}{2} \le \xi \le \frac{3}{4} \\ \frac{272}{7}\xi^3 - \frac{816}{7}\xi^2 + \frac{771}{7}\xi - \frac{227}{7} & if\ \frac{3}{4} \le \xi \le 1 \end{cases} \quad (16)$$

In the direction of y

$$Y_1(\eta) = \begin{cases} -\frac{272}{7}\eta^3 + \frac{45}{7}\eta & if\ 0 \le \eta \le \frac{1}{4} \\ \frac{464}{7}\eta^3 - \frac{552}{7}\eta^2 + \frac{183}{7}\eta - \frac{23}{14} & if\ \frac{1}{4} \le \eta \le \frac{1}{2} \\ -\frac{240}{7}\eta^3 + 72\eta^2 - \frac{345}{7}\eta + \frac{153}{14} & if\ \frac{1}{2} \le \eta \le \frac{3}{4} \\ \frac{48}{7}\eta^3 - \frac{144}{7}\eta^2 + \frac{141}{7}\eta - \frac{45}{7} & if\ \frac{3}{4} \le \eta \le 1 \end{cases} \quad (17)$$

$$Y_2(\eta) = \begin{cases} \frac{192}{7}\eta^3 - \frac{12}{7}\eta & if\ 0 \le \eta \le \frac{1}{4} \\ -\frac{512}{7}\eta^3 + \frac{528}{7}\eta^2 - \frac{144}{7}\eta + \frac{11}{7} & if\ \frac{1}{4} \le \eta \le \frac{1}{2} \\ \frac{512}{7}\eta^3 - 144\eta^2 + \frac{624}{7}\eta - \frac{117}{7} & if\ \frac{1}{2} \le \eta \le \frac{3}{4} \\ -\frac{192}{7}\eta^3 + \frac{576}{7}\eta^2 - \frac{564}{7}\eta + \frac{180}{7} & if\ \frac{3}{4} \le \eta \le 1 \end{cases} \quad (18)$$

$$Y_3(\eta) = \begin{cases} -\frac{48}{7}\eta^3 + \frac{3}{7}\eta & if\ 0 \le \eta \le \frac{1}{4} \\ \frac{240}{7}\eta^3 - \frac{216}{7}\eta^2 + \frac{57}{7}\eta - \frac{9}{14} & if\ \frac{1}{4} \le \eta \le \frac{1}{2} \\ -\frac{464}{7}\eta^3 + 120\eta^2 - \frac{471}{7}\eta + \frac{167}{14} & if\ \frac{1}{2} \le \eta \le \frac{3}{4} \\ \frac{272}{7}\eta^3 - \frac{816}{7}\eta^2 + \frac{771}{7}\eta - \frac{227}{7} & if\ \frac{3}{4} \le \eta \le 1 \end{cases} \quad (19)$$

❖ Consideration of five strips in the directions of x and y respectively:

In the direction of x

© 2024 by the author(s). Licensee NIJOTECH.
This article is open access under the CC BY-NC-ND license.
http://creativecommons.org/licenses/by-nc-nd/4.0/

$$X_1(\xi)=\begin{cases}-\frac{15875}{209}\xi^3+\frac{1680}{209}\xi & if\ 0\le\xi\le\frac{1}{5}\\ \frac{27125}{209}\xi^3-\frac{25800}{209}\xi^2+\frac{360}{11}\xi-\frac{344}{209} & if\ \frac{1}{5}\le\xi\le\frac{2}{5}\\ -\frac{750}{11}\xi^3+\frac{23850}{209}\xi^2-\frac{13020}{209}\xi+\frac{2304}{209} & if\ \frac{2}{5}\le\xi\le\frac{3}{5}\\ \frac{3750}{209}\xi^3-\frac{450}{11}\xi^2+\frac{6420}{209}\xi-\frac{144}{19} & if\ \frac{3}{5}\le\xi\le\frac{4}{5}\\ -\frac{750}{209}\xi^3+\frac{2250}{209}\xi^2-\frac{2220}{209}\xi+\frac{720}{209} & if\ \frac{4}{5}\le\xi\le 1\end{cases}\quad(20)$$

$$X_2(\xi)=\begin{cases}\frac{11250}{209}\xi^3-\frac{450}{209}\xi & if\ 0\le\xi\le\frac{1}{5}\\ -\frac{30125}{209}\xi^3+\frac{24825}{209}\xi^2-\frac{285}{11}\xi+\frac{331}{209} & if\ \frac{1}{5}\le\xi\le\frac{2}{5}\\ \frac{1625}{11}\xi^3-\frac{48375}{209}\xi^2+\frac{23865}{209}\xi-\frac{3573}{209} & if\ \frac{2}{5}\le\xi\le\frac{3}{5}\\ -\frac{15000}{209}\xi^3+\frac{1800}{11}\xi^2-\frac{25680}{209}\xi+\frac{576}{19} & if\ \frac{3}{5}\le\xi\le\frac{4}{5}\\ \frac{3000}{209}\xi^3-\frac{9000}{209}\xi^2+\frac{8880}{209}\xi-\frac{2880}{209} & if\ \frac{4}{5}\le\xi\le 1\end{cases}\quad(21)$$

$$X_3(\xi)=\begin{cases}-\frac{3000}{209}\xi^3+\frac{120}{209}\xi & if\ 0\le\xi\le\frac{1}{5}\\ \frac{1500}{209}\xi^3-\frac{10800}{209}\xi^2+\frac{120}{11}\xi-\frac{144}{209} & if\ \frac{1}{5}\le\xi\le\frac{2}{5}\\ -\frac{1625}{11}\xi^3+\frac{44250}{209}\xi^2-\frac{19740}{209}\xi+\frac{2792}{209} & if\ \frac{2}{5}\le\xi\le\frac{3}{5}\\ \frac{30125}{209}\xi^3-\frac{3450}{11}\xi^2+\frac{46140}{209}\xi-\frac{944}{19} & if\ \frac{3}{5}\le\xi\le\frac{4}{5}\\ -\frac{11250}{209}\xi^3+\frac{33750}{209}\xi^2-\frac{33300}{209}\xi+\frac{10800}{209} & if\ \frac{4}{5}\le\xi\le 1\end{cases}\quad(22)$$

$$X_4(\xi)=\begin{cases}\frac{750}{209}\xi^3-\frac{30}{209}\xi & if\ 0\le\xi\le\frac{1}{5}\\ -\frac{3750}{209}\xi^3+\frac{2700}{209}\xi^2-\frac{30}{11}\xi+\frac{36}{209} & if\ \frac{1}{5}\le\xi\le\frac{2}{5}\\ \frac{750}{11}\xi^3-\frac{18900}{209}\xi^2+\frac{8070}{209}\xi-\frac{1116}{209} & if\ \frac{2}{5}\le\xi\le\frac{3}{5}\\ -\frac{27125}{209}\xi^3+\frac{2925}{11}\xi^2-\frac{36615}{209}\xi+\frac{711}{19} & if\ \frac{3}{5}\le\xi\le\frac{4}{5}\\ \frac{15875}{209}\xi^3-\frac{47625}{209}\xi^2+\frac{45945}{209}\xi-\frac{14195}{209} & if\ \frac{4}{5}\le\xi\le 1\end{cases}\quad(23)$$

In the direction of y

$$Y_1(\eta)=\begin{cases}-\frac{15875}{209}\eta^3+\frac{1680}{209}\eta & if\ 0\le\eta\le\frac{1}{5}\\ \frac{27125}{209}\eta^3-\frac{25800}{209}\eta^2+\frac{360}{11}\eta-\frac{344}{209} & if\ \frac{1}{5}\le\eta\le\frac{2}{5}\\ -\frac{750}{11}\eta^3+\frac{23850}{209}\eta^2-\frac{13020}{209}\eta+\frac{2304}{209} & if\ \frac{2}{5}\le\eta\le\frac{3}{5}\\ \frac{3750}{209}\eta^3-\frac{450}{11}\eta^2+\frac{6420}{209}\eta-\frac{144}{19} & if\ \frac{3}{5}\le\eta\le\frac{4}{5}\\ -\frac{750}{209}\eta^3+\frac{2250}{209}\eta^2-\frac{2220}{209}\eta+\frac{720}{209} & if\ \frac{4}{5}\le\eta\le 1\end{cases}\quad(24)$$

$$Y_2(\eta)=\begin{cases}\frac{11250}{209}\eta^3-\frac{450}{209}\eta & if\ 0\le\eta\le\frac{1}{5}\\ -\frac{30125}{209}\eta^3+\frac{24825}{209}\eta^2-\frac{285}{11}\eta+\frac{331}{209} & if\ \frac{1}{5}\le\eta\le\frac{2}{5}\\ \frac{1625}{11}\eta^3-\frac{48375}{209}\eta^2+\frac{23865}{209}\eta-\frac{3573}{209} & if\ \frac{2}{5}\le\eta\le\frac{3}{5}\\ -\frac{15000}{209}\eta^3+\frac{1800}{11}\eta^2-\frac{25680}{209}\eta+\frac{576}{19} & if\ \frac{3}{5}\le\eta\le\frac{4}{5}\\ \frac{3000}{209}\eta^3-\frac{9000}{209}\eta^2+\frac{8880}{209}\eta-\frac{2880}{209} & if\ \frac{4}{5}\le\eta\le 1\end{cases}\quad(25)$$

$$Y_3(\eta)=\begin{cases}-\frac{3000}{209}\eta^3+\frac{120}{209}\eta & if\ 0\le\eta\le\frac{1}{5}\\ \frac{1500}{209}\eta^3-\frac{10800}{209}\eta^2+\frac{120}{11}\eta-\frac{144}{209} & if\ \frac{1}{5}\le\eta\le\frac{2}{5}\\ -\frac{1625}{11}\eta^3+\frac{44250}{209}\eta^2-\frac{19740}{209}\eta+\frac{2792}{209} & if\ \frac{2}{5}\le\eta\le\frac{3}{5}\\ \frac{30125}{209}\eta^3-\frac{3450}{11}\eta^2+\frac{46140}{209}\eta-\frac{944}{19} & if\ \frac{3}{5}\le\eta\le\frac{4}{5}\\ -\frac{11250}{209}\eta^3+\frac{33750}{209}\eta^2-\frac{33300}{209}\eta+\frac{10800}{209} & if\ \frac{4}{5}\le\eta\le 1\end{cases}\quad(26)$$

$$Y_4(\eta)=\begin{cases}\frac{750}{209}\eta^3-\frac{30}{209}\eta & if\ 0\le\eta\le\frac{1}{5}\\ -\frac{3750}{209}\eta^3+\frac{2700}{209}\eta^2-\frac{30}{11}\eta+\frac{36}{209} & if\ \frac{1}{5}\le\eta\le\frac{2}{5}\\ \frac{750}{11}\eta^3-\frac{18900}{209}\eta^2+\frac{8070}{209}\eta-\frac{1116}{209} & if\ \frac{2}{5}\le\eta\le\frac{3}{5}\\ -\frac{27125}{209}\eta^3+\frac{2925}{11}\eta^2-\frac{36615}{209}\eta+\frac{711}{19} & if\ \frac{3}{5}\le\eta\le\frac{4}{5}\\ \frac{15875}{209}\eta^3-\frac{47625}{209}\eta^2+\frac{45945}{209}\eta-\frac{14195}{209} & if\ \frac{4}{5}\le\eta\le 1\end{cases}\quad(27)$$

Similar trial functions were derived for the following sets of plate's classical boundary conditions:

- ✓ Simple supports at three sides and one edge fixed (SSSC)
- ✓ Simple supports at two adjacent sides and the other two edges fixed (SSCC)
- ✓ A simple support at one side and the other three edges fixed (SCCC)
- ✓ all-round fixed (CCCC)

2.2 Ritz Procedure

Adopting $\xi=\frac{x}{a}$ and $\eta=\frac{y}{b}$, the maximum strain energy of an isotropic thin rectangular plate is given as [9]:

$$U_{max}=\frac{1}{2}\frac{Db}{a^3}\int_0^1\int_0^1[W_{\xi\xi}^2+\alpha^4W_{\eta\eta}^2+2\mu\alpha^2W_{\xi\xi}W_{\eta\eta}+2(1-\mu)\alpha^2W_{\xi\eta}^2]d\xi d\eta \quad (28)$$

Where, a and b are the dimension of the plate, W its transverse displacement function, D its flexural rigidity, μ the Poisson's ratio of its material, α its aspect ratio, the subscripts ξ and η stand for first differentiation with respect to ξ and η respectively, and the subscripts ξξ and ηη stand for second differentiation with respect to ξ and η respectively.

The maximum kinetic energy is given by:

$$T_{max}=\frac{1}{2}\omega^2\rho hab\int_0^1\int_0^1W^2(\xi,\eta)d\xi d\eta \quad (29)$$

Where, ρ refers to the mass density of the material of the plate.

Considering the plate to be under free vibration, its energy functional will obtained as:

$$\Pi=U_{max}-T_{max} \quad (30)$$

We assume the shape function to be in the following form:

$$W(\xi,\eta)=\sum_i^m\sum_j^n C_{ij}X_i(\xi)Y_j(\eta) \quad (31)$$

Where, C_{ij} are undetermined coefficients corresponding to the nodal displacements in Equation (1) and, $X_i(\xi)$ and $Y_j(\eta)$ are the piecewise polynomial functions as derived in Section 2.1, and n and m are the numbers of trial functions (or of strips) considered the directions of x and y respectively. Substituting for the expression of $X_i(\xi)$ and $Y_j(\eta)$ into Equation (28) and Equation (29), and taking into account Equation (30), we will obtain a system of algebraic equations in the undetermined coefficients C_{ij}, after minimisation of the energy functional Π:

$$\frac{\partial\Pi}{\partial C_{ij}}=0 \quad (32)$$

Adopting matrix formats, the plate's energy functional itself can be written as [9]:

$$\Pi=\frac{1}{2}\frac{Db}{a^3}C[A_1+\alpha^4A_2+2\mu\alpha^2A_3+2(1-\mu)\alpha^2A_4-\lambda^2B]C^T \quad (33)$$

Where,

$A_1=\int_0^1\int_0^1M_{\xi\xi}^TM_{\xi\xi}d\xi d\eta$; $A_2=\int_0^1\int_0^1M_{\eta\eta}^TM_{\eta\eta}d\xi d\eta$; $A_3=\int_0^1\int_0^1M_{\eta\eta}^TM_{\xi\xi}d\xi d\eta$; $A_4=\int_0^1\int_0^1M_{\xi\eta}^TM_{\xi\eta}d\xi d\eta$; $B=\int_0^1\int_0^1M^TMd\xi d\eta$

and $\lambda^2=\frac{\rho h\omega^2a^4}{D}$

© 2024 by the author(s). Licensee NIJOTECH.
This article is open access under the CC BY-NC-ND license.
http://creativecommons.org/licenses/by-nc-nd/4.0/

Carrying out the minimisation suggested by Equation (32), we have:

$$HC^T = 0 \quad (34)$$

Where, $H = [A_1 + \alpha^4 A_2 + 2\mu\alpha^2 A_3 + 2(1-\mu)\alpha^2 A_4 - \lambda^2 B]$

A₁, A₂, A₃, A₄ and B are computed as:

$$A_1 = \int_0^1\int_0^1 M_{\xi\xi}^T M_{\xi\xi} d\xi d\eta = \int_0^1\int_0^1 \begin{bmatrix} w_{1\xi\xi}w_{1\xi\xi} & w_{1\xi\xi}w_{2\xi\xi} & \cdots & w_{1\xi\xi}w_{p\xi\xi} \\ w_{2\xi\xi}w_{1\xi\xi} & w_{2\xi\xi}w_{2\xi\xi} & \cdots & w_{2\xi\xi}w_{p\xi\xi} \\ . & . & \cdots & . \\ . & . & \cdots & . \\ . & . & \cdots & . \\ w_{p\xi\xi}w_{1\xi\xi} & w_{p\xi\xi}w_{2\xi\xi} & \cdots & w_{p\xi\xi}w_{p\xi\xi} \end{bmatrix} \quad (35)$$

$$A_2 = \int_0^1\int_0^1 M_{\eta\eta}^T M_{\eta\eta} d\xi d\eta = \int_0^1\int_0^1 \begin{bmatrix} w_{1\eta\eta}w_{1\eta\eta} & w_{1\eta\eta}w_{2\eta\eta} & \cdots & w_{1\eta\eta}w_{p\eta\eta} \\ w_{2\eta\eta}w_{1\eta\eta} & w_{2\eta\eta}w_{2\eta\eta} & \cdots & w_{2\eta\eta}w_{p\eta\eta} \\ . & . & \cdots & . \\ . & . & \cdots & . \\ . & . & \cdots & . \\ w_{p\eta\eta}w_{1\eta\eta} & w_{p\eta\eta}w_{2\eta\eta} & \cdots & w_{p\eta\eta}w_{p\eta\eta} \end{bmatrix} \quad (36)$$

$$A_3 = \int_0^1\int_0^1 M_{\eta\eta}^T M_{\xi\xi} d\xi d\eta = \int_0^1\int_0^1 \begin{bmatrix} w_{1\eta\eta}w_{1\xi\xi} & w_{1\eta\eta}w_{2\xi\xi} & \cdots & w_{1\eta\eta}w_{p\xi\xi} \\ w_{2\eta\eta}w_{1\xi\xi} & w_{2\eta\eta}w_{2\xi\xi} & \cdots & w_{2\eta\eta}w_{p\xi\xi} \\ . & . & \cdots & . \\ . & . & \cdots & . \\ . & . & \cdots & . \\ w_{p\eta\eta}w_{1\xi\xi} & w_{p\eta\eta}w_{2\xi\xi} & \cdots & w_{p\eta\eta}w_{p\xi\xi} \end{bmatrix} \quad (37)$$

$$A_4 = \int_0^1\int_0^1 M_{\xi\eta}^T M_{\xi\eta} d\xi d\eta = \int_0^1\int_0^1 \begin{bmatrix} w_{1\xi\eta}w_{1\xi\eta} & w_{1\xi\eta}w_{2\xi\eta} & \cdots & w_{1\xi\eta}w_{p\xi\eta} \\ w_{2\xi\eta}w_{1\xi\eta} & w_{2\xi\eta}w_{2\xi\eta} & \cdots & w_{2\xi\eta}w_{p\xi\eta} \\ . & . & \cdots & . \\ . & . & \cdots & . \\ . & . & \cdots & . \\ w_{p\xi\eta}w_{1\xi\eta} & w_{p\xi\eta}w_{2\xi\eta} & \cdots & w_{p\xi\eta}w_{p\xi\eta} \end{bmatrix} \quad (38)$$

$$B = \int_0^1\int_0^1 M^T M d\xi d\eta = \int_0^1\int_0^1 \begin{bmatrix} w_1w_1 & w_1w_2 & \cdots & w_1w_p \\ w_2w_1 & w_2w_2 & \cdots & w_2w_p \\ . & . & \cdots & . \\ . & . & \cdots & . \\ . & . & \cdots & . \\ w_pw_1 & w_pw_2 & \cdots & w_pw_p \end{bmatrix} \quad (39)$$

An eigenvalue problem is obtained upon application of Equation (34). The condition of non-trivial solution requires that the determinant of H should be null. This leads to a polynomial equation whose solution gives λ called frequency parameter.

3.0 RESULTS AND DISCUSSION

3.1 The Trial Functions

Polynomial piecewise comparison functions were constructed from consistent deflection patterns conveniently imposed to the plate structures for boundary conditions comprising simple and/or fixed supports. In fact, they can be constructed for any combination of classical plate's edge conditions. The derived trial functions are all three-degree polynomials. The use of these low-degree polynomials will help to avoid the numerical instability and wiggling associated with the use of high degree polynomials during the implementation of the Ritz procedure [6], [10].

The Ritz method was implemented using Mathematica software for SSSS, SSSC, SSCC, SCCC and CCCC thin rectangular plates considering successively two, three and four equal strips in the directions of x and y, and varying the plates' side ratios (1, 1.5, 2 and 2.5). The Poisson's ratio μ of the plates' material was taken equal to 0.3. The numerical results for the six first frequency parameters λ were retained and compared to existing results as shown in Tables 1, 2, 3, 4 and 5. The percentage differences presented in the tables are computed using the formula:

$$Percentage\ difference = \frac{value\ from\ reference - value\ from\ present\ study}{value\ from\ reference}$$

Table 1: Frequency parameters for SSSS rectangular isotropic plates of different side ratios compared with existing results

Side ratio		λ for the modes of vibration					
		1	2	3	4	5	6
1	Present study	19.7404 (-0.066)* (-0.007)**	49.4283 (-0.211)* (-0.163)**	49.4283 (-0.211)* (-0.163)**	79.0644 (-0.228)* (-0.136)**	100.21 (-1.671)* (-1.534)**	100.21 (-1.671)* (-1.534)**
	[11]	19.7273	49.3242	49.3242	78.8848	98.5628	98.5628
	Exact value (Navier's solution)	19.739	49.348	49.348	78.957	98.696	98.696
1.5	Present study	32.0784 (-0.749)* (-0.007)**	61.7521 (-0.655)* (-0.109)**	98.896 (-1.328)* (-0.203)**	112.432 (-1.721)* (-1.260)**	128.501 (-1.097)* (-0.153)**	178.824 - (-0.659)**
	[12]	31.8400	61.3500	97.60	110.5300	127.1070	-
	Exact value (Navier's solution)	32.0762	61.685	98.696	111.033	128.305	177.653
2	Present study	49.352 (-0.008)* (-0.008)**	79.013 (-0.071)* (-0.071)**	129.58 (0.077)* (-0.994)**	168.153 (0.159)* (-0.221)**	197.74 (0.448)* (-0.176)**	208.953 - (-5.857)**
	[13]	49.348	78.957	129.68	168.42	198.63	-
	Exact value (Navier's solution)	49.348	78.9568	128.305	167.783	197.392	197.392
2.5	Present study	71.5611 (-0.226)* (-0.009)**	101.212 (-0.289)* (-0.048)**	151.67 (-1,081)* (-0.770)**	230.773 (-5.520)* (-5.088)**	257.198 (-0.692)* (-0.229)**	286.775 - (-0.194)**
	[12]	71.4000	100.92	150.048	218.70	255.4300	-
	Exact value (Navier's solution)	71.5546	101.163	150.511	219.599	256.61	286.219

* *Percentage difference comparatively to [11], [12] or [13]*

© 2024 by the author(s). Licensee NIJOTECH.
This article is open access under the CC BY-NC-ND license.
http://creativecommons.org/licenses/by-nc-nd/4.0/

**Percentage difference comparatively to Navier's solution*

Table 2: Frequency parameters for SSSC rectangular isotropic plates of different side ratios compared with existing results

Side ratio		λ for the modes of vibration					
		1	2	3	4	5	6
1	Present study	23.6517 (-0.024)* (-0.024)**	51.7697 (-0.185)* (-0.183)*	58.8202 (-0.297)* (-0.295)**	86.3402 (-0.244)* (-0.237)**	101.811 (-1.540)* (-1.535)**	115.68 (-2.165)* (-2.161)**
	Exact value [14]	23.646	51.674	58.646	86.130	100.267	113.229
	[6]	23.646	51.675	58.647	86.136	100.272	113.233
1.5	Present study	42.5372 (-0.022)* (0.374)**	69.0793 (-0.110)* (-1.620)**	117.654 (-1.193)* (-1.765)**	121.42 (-0.351)* (-2.269)**	148.029 (-0.267)* -	195.132 (-5.992)* -
	[15]	42.5278	69.0031	116.2671	120.9956	147.6353	184.1006
	[16]	42.697	67.978	115.613	118.726	-	-
2	Present study	69.3436 (-0.021)* (-0.024)**	94.6501 (-0.073)* (-0.060)**	141.424 (-0.871)* (-0.031)**	209.172 (-1.197)* -	217.97 (-4.589)* (-4.572)**	235.303 (-0.304)* -
	Exact value [14]	69.329	94.581	140.203	206.698	208.407	234.589
	[13]	69.327	94.593	141.38	-	208.44	-
2.5	Present study	103.949 (-0.025)*	128.4 (-0.048)*	173.45 (-0.620)*	247.903 (-4.490)*	322.033 (-0.387)*	347.898 (-0.334)*
	[15]	103.9227	128.3382	172.3804	237.2502	320.7921	346.7382

* *Percentage difference comparatively to [14] or [15]*
***Percentage difference comparatively to [6], [13] or [16]*

Table 3: Frequency parameters for SSCC rectangular isotropic plates of different side ratios compared with existing results

Side ratio		λ for the modes of vibration					
		1	2	3	4	5	6
1	Present study	27.065 (-0.037)* (-0.041)**	60.7292 (-0.296)* (-0.313)**	60.9737 (-0.700)* (-0.307)**	93.1432 (-0.247)* (-0.327)**	117.032 (-1.732)* (-2.156)**	117.176 - (-2.151)**
	[13]	27.055	60.550	60.550	92.914	115.04	-
	[6]	27.054	60.540	60.787	92.840	114.562	114.709
1.5	Present study	44.9106 (-0.039)* (-2.095)**	76.7128 (-0.207)* (-0.612)**	122.787 (-0.374)* (0.307)**	131.651 (-1.732)* (-4.404)**	153.095 (-0.338)* -	205.711 (-1.505)* -
	[15]	44.893	76.554	122.33	129.41	152.58	202.66
	[16]	43.989	76.246	123.167	126.098	-	-
2	Present study	71.113 (-0.049)*	100.963 (-0.162)*	153.934 (-1.126)*	210.23 (-0.368)*	235.88 (-0.911)*	239.358 -
	[13]	71.078	100.80	152.22	209.46	233.75	-
2.5	Present study	105.356 (-0.044)*	133.681 (-0.121)*	184.525 (-0.982)*	264.685 (-4.544)*	322.921 (-0.411)*	351.332 (-1.989)*
	[15]	105.31	133.52	182.73	253.18	321.60	344.48

* *Percentage difference comparatively to [13] or [15]*
***Percentage difference comparatively to [6], or [16]*

Table 4: Frequency parameters for SCCC rectangular isotropic plates of different side ratios compared with existing results

Side ratio		λ for the modes of vibration					
		1	2	3	4	5	6
1	Present study	31.8479 (-0.088)* (-0.059)** (-0.069)***	63.5474 (-0.359)* (-0.316)** (-0.342)***	71.4298 (-0.492)* (-0.486)** (-0.498)***	101.256 (-0.452)* (-0.422)** (-0.460)***	118.871 (-2.158)* (-2.123)** (-2.161)***	133.94 (-2.715)* (-2.738)** (-2.753)***
	[17]	31.82	63.32	71.08	100.8	116.36	130.4
	[15]	31.829	63.347	71.084	100.83	116.40	130.37
	[18]	31.826	63.331	71.076	100.792	116.357	130.351
1.5	Present study	58.2235 (-0.058)*	85.9016 (-0.224)*	137.927 (-1.641)*	148.259 (-0.583)*	175.36 (-0.550)*	219.445 (- 5.859)*
	[17]	58.19	85.71	135.7	147.4	174.4	207.3
2	Present study	96.6412 (-0.032)*	121.192 (-0.159)*	168.961 (-1.174)*	247.058 (-4.952)*	256.549 (-0.607)*	282.213 (-0.575)*
	[17]	96.61	121.0	167.0	235.4	255.0	280.6
2.5	Present study	146.603 (-0.070)*	169.081 (-0.107)*	212.895 (-0.803)*	286.695 (-3.988)*	396.03 (-0.643)*	420.9 (-0.622)*

© 2024 by the author(s). Licensee NIJOTECH.
This article is open access under the CC BY-NC-ND license.
http://creativecommons.org/licenses/by-nc-nd/4.0/

	[17]	146.5	168.9	211.2	275.7	393.5	418.3

* *Percentage difference comparatively to [17]*
***Percentage difference comparatively to [15]*
*** *Percentage difference comparatively to [18]*

Table 5: Frequency parameters for CCCC rectangular isotropic plates of different side ratios compared with existing results

Side Ratio		**λ for the modes of vibration**					
		1	2	3	4	5	6
1	Present Study	36.0197 (-0.082)* (-0.093)**	73.7727 (-0.508)* (-0.512)**	73.7727 (-0.508)* (-0.512)**	108.835 (-0.587)* (-0.564)**	135.217 (-2.748)* (-2.755)**	135.816 (-2.735)* (-2.724)**
	[19]	35.99	73.40	73.40	108.2	131.6	132.2
	[6]	35.986	73.397	73.397	108.225	131.592	132.215
1.5	Present Study	60.8214 (-0.101)* (-0.081)**	94.1747 (-0.357)* (-0.335)**	149.705 (-0.608)* (-0.595)**	152.992 (-2.199)* (-2.172)**	180.699 (-0.612)* (-0.578)**	234.829 (-3.540)* (-3.485)**
	[19]	60.76	93.84	148.8	149.7	179.6	226.8
	[20]	60.772	93.860	148.82	149.74	179.66	226.92
2	Present Study	98.4116 (-0.103)* (-0.096)**	127.655 (-0.279)* (-0.271)**	182.066 (-1.656)* (-1.560)**	257.617 (-1.704)* (-1.269)**	261.645 (-2.245)* (-2.197)**	286.299 (-0.703)*
	[19]	98.31	127.3	179.1	253.3	255.9	284.3
	[13]	98.317	127.31	179.27	254.39	256.02	-
2.5	Present Study	147.927 (-0.086)* (-0.086)**	174.203 (-0.232)* (-0.203)**	224.085 (-1.213)* (-1.149)**	300.293 (-2.946)* (-2.879)**	396.907 (-0.661)* (-0.643)**	424.278
	[19]	147.8	173.8	221.4	291.7	394.3	-
	[15]	147.80	173·85	221.54	291.89	394.37	-

* *Percentage difference comparatively to [19]*
***Percentage difference comparatively to [6], [13], [15] or [20]*

3.2 Comparison with Existing Exact Solutions

Free vibration exact solutions for thin rectangular plates exist for SSSS and SSSC boundary conditions. So, they can be used as benchmarks for verifying the real accuracy of the approach used in the present work.

(i) **SSSS plates** (Table 1): The first six frequency parameters obtained using the constructed polynomial comparison functions were 19.7404, 49.4283, 49.4283, 79.0644, 100.21 and 100.21 respectively for a simply supported square plate (aspect ratio = 1). When compared to the exact Navier's solutions, they showed a very high accuracy as the percentage differences ranged from - 0.007% (for the fundamental mode) to - 1.534% (for the sixth mode). Similar trends were observed for the other aspect ratios considered. For all the plate's side ratios considered, the percentage differences remained less than 1% for the first three modes comparatively to exact solutions. The computed results were also in accordance with other approximate solutions from other references [11], [12], [13].

(ii) **SSSC plates** (Table 2): The first six frequency parameters computed for an SSSC square plate were 23.6517, 51.7697, 58.8202, 86.3402, 101.811 and 115.68 respectively, exhibiting percentage differences varying from - 0.024% for the fundamental frequency parameter to - 2.165% for the sixth frequency parameter, when compared to exact solutions by Wang C. Y. and Wang C. M. [14]. Similarly, the computed frequency parameters for the plate's aspect ratio of 2 were in good agreement with the corresponding exact solutions from the same authors. Similar consistent results were also observed throughout the plate side ratios considered comparatively to approximate numerical values of frequency parameters within the six first modes computed by other researchers [6], [13], [15], [16].

3.3 SSCC, SCCC and CCCC Rectangular Plates

There exist no exact solutions for the dynamic study of thin rectangular under the SSCC, SCCC and CCCC boundary conditions. However considerable approximate solutions are available in the literature for assessing the results of the present work.

(i) **SSCC thin plates** (Table 3): When the derived piecewise polynomial comparison functions were used, the first six frequency parameters obtained for an SSCC square plate were 27.065, 60.7292, 60.9737, 93.1432, 117.032 and 117.176. They exhibited a very good accuracy comparatively to the results obtained by Chakraverty [13] and Monterrubio and Ilanko [6]: the percentage differences were confined between - 0.037% and - 2.156%. For the other aspect ratios studied, the results remained consistent with those available in the literature [13], [15], [16].

(ii) **SCCC thin plates** (Table 4): the frequency parameters obtained for an SCCC square thin

© 2024 by the author(s). Licensee NIJOTECH.
This article is open access under the CC BY-NC-ND license.
http://creativecommons.org/licenses/by-nc-nd/4.0/

plate using the present polynomial comparison functions were 31.8479, 63.5474, 71.4298, 101.256, 118.871 and 133.94 respectively, showing percentage differences between - 0.059% and - 2.763% comparatively to existing solutions [15], [17], [18]. Table 4 shows a good concordance between the results computed herein and those obtained by Gorman [17] throughout the six modes retained and the four aspect ratios considered for SCCC thin rectangular plates.

(iii) CCCC thin plates (Table 5): When the polynomial shape functions were used, the obtained six frequency parameters for a clamped square thin plate were 36.0197, 73.7727, 73.7727, 108.835, 135.217 and 135.816 respectively, which were found to be in concordance with those given by Li [19], and Monterrubio and Ilanko [6]: the percentage differences ranged from - 0.082% to - 2.755%. Similarly, it was observed a good agreement between the present results and available solutions for 1.5, 2 and 2.5 plate side ratios as the percentage differences obtained were as low as - 0.081% and did not go beyond - 3.54% across the six modes considered for each of the cases [13], [15], [19], [20].

Finally, the following observations which cut across the five sets of rectangular plates boundary conditions considered in this work could be made:

- ✓ There is a decreasing accuracy in the calculated frequency parameters as they move from the lower to the higher modes.
- ✓ For each of the modes considered, there is a consistent increment in the computed frequency parameters with the number of fixed edges in the set of plate boundary conditions. As an illustration, the fundamental frequency parameter varied from 19.7273 for a simply supported square plate to 36.0197 for a clamped square plate.
- ✓ The frequency parameter increased with the rectangular plate's side ratio for a given combinations of edge supports.

4.0 CONCLUSION

In this study, piecewise polynomial trial functions to be used for the dynamic analysis of thin rectangular plates were constructed from imposed plate deflection patterns adopting the Ritz procedure. In fact, they can be derived for all the classical boundary conditions, and have a degree low enough to avoid numerical instability during the implementation of the Ritz procedure. The method was applied considering 2, 3 and 4 strips in the two perpendicular directions of the plate and the six first modes were retained, tabulated and compared to existing results for SSSS, SSSC, SSCC, SCCC and CCCC boundary conditions. Four plate aspect ratios were taken into account namely 1, 1.5, 2 and 2.5.

To assess the reliability of the trial functions so constructed, the results were first compared to existing exact solutions for SSSS and SSSC plate boundary conditions and they were found to be accurate. The results for the other sets of boundary conditions (SSCC, SCCC and CCCC) were also consistent with those of other researchers.

For each of the modes considered, it was observed a consistent increment in the computed frequency parameters as the number of clamped edges increased in the set of plate boundary conditions. The practical consequence is that thin rectangular plates with clamped edges may witness resonance when subjected to high forcing frequencies, while they can resist the low and medium ones.

REFERENCES

[1] Verma, Y., and Datta, N. "Comprehensive Study of Free Vibration of Rectangular Mindlin's Plates with Rotationally Constrained Edges Using Dynamic Timoshenko Trial Functions", *Engng. Trans.*, vol. 66, no. 2, 2007, pp. 129-160, 2018.

[2] Wafa, A. S. and Riyam A. D. "Vibration Response of Free and Force Analysis of a Rectangular Plate", *Journal of University of Babylon for Engineering Sciences*, vol. 26, no. 8, pp. 298-308, 2018.

[3] Wu, T., Chen, Z. B. and Qu, J. J. "A Modified Fourier-Ritz Method for Free Vibration of Rectangular Plates with Elastic Constrains", *Journal of Theoretical and Applied Mechanics*, vol. 60, no. 1, pp. 77-89, 2022.

[4] Ramu, I. and Mohanty, S. C. "Vibration of Rectangular Plates by Reduction of the Plate Partial Differential Equation into Simultaneous Ordinary Differential Equations", *Procedia Engineering*, vol. 38, pp. 2758-2766, 2012.

[5] Brown, R. E. and Stone, M. A. "On the Use of Polynomial Series with Rayleigh-Ritz Method", *Composite Structures*, vol. 39, no. 3-4, pp. 191-196, 1997.

[6] Monterrubio, L. E. and Ilanko, S. "Sets of admissible functions for the Rayleigh-Ritz method", in *Proceeding of the Eleventh International Conference on Computational Structures Technology, 4-7 September*, B. H. V. Topping, Ed. Dubrovnik: Civil-Comp. Press, 2012, pp. 1511-1526.

© 2024 by the author(s). Licensee NIJOTECH.
This article is open access under the CC BY-NC-ND license.
http://creativecommons.org/licenses/by-nc-nd/4.0/

[7] Adah E. I., Ibearugbulem, O. M., Onwuka, D. O. and Okoroafor, S. U. "Determination of Resonating Frequency of Thin Rectangular Flat Plates", *International Journal of Civil and Structural Engineering Research*, vol. 7, no. 1, pp. 16-22, 2019.

[8] Asomugha, A. U., Onyeka, J. O. and Opara, H. E. "Free Vibration Analysis of CSCS & CSSS Rectangular Plate by Split-deflection Method", *International Journal of Engineering & Scientific Research*, vol. 7, no. 5, pp. 21-42, 2019.

[9] Aginam C. H., Adamou A. and Nwaiwu C. M. O. "Free Vibration Analysis of all round Clamped Thin Isotropic Rectangular Plate by Ritz Direct Variational Method", *Nigerian Journal of Technology (NIJOTECH)*, vol. 40, no. 6, pp.1030-1038, 2021.

[10] Jaworski, J. W. and Dowell, E. H. "Free Vibration of a Cantilevered Beam with Multiple Steps: Comparison of Several Theoretical Methods with Experiment", *Journal of Sound and Vibration*, vol. 312, 713-725, 2008.

[11] Dal, H., and Morgul O. K. "Vibration of Elastically Restrained Rectangular Plates", *Scientific Research and Essays*, vol. 6, no. 34, pp. 6911-6816, 2011.

[12] Abdul-Razzak, A. A. and Haido, J. H. "Free Vibration Analysis of Rectangular Plates Using Higher Order Finite Layer Method", *Al-Rafidain Engineering*, vol. 15, no. 3, 19-32, 2007

[13] Chakraverty, S. *Vibration of Plates*, CRC Press, Taylor & Francis Group, New York, 2009.

[14] Wang C. Y. and Wang, C. M. *Structural Vibration: Exact Solutions for Strings, Membranes, Beams and Plates*, CRC Press, Taylor & Francis Group, New York, 2014.

[15] Leissa A. W. "The Free Vibration of Rectangular Plates", *Journal of Sound and Vibration*, vol. 31, no. 3, pp. 257-293, 1973.

[16] Yousef S. A. and Osama A. "Free and forced vibration of rectangular plates using the finite difference method", in *Green Building, Materials and Civil Engineering*, Jimmy C.M. Kao, Wen-Pei Sung and Ran Chen, Eds. London: CRC Press, Taylor & Francis Group, 2015, pp. 627-633.

[17] Gorman, D. J. *Free Vibration Analysis of Rectangular Plates*, Elsevier, Amsterdam, 1982

[18] Eftekhari, S. A. and Jafari, A. A. "A Mixed Method for Free and Forced Vibration of Rectangular Plates", *Applied Mathematical Modelling*, vol. 36, pp. 2814-2831, 2012.

[19] Li, W. L. "Vibration Analysis of Rectangular Plates with General Elastic Boundary Supports", *Journal of Sound and Vibration*, vol. 273, no. 3, pp. 619-635, 2004.

[20] Bhat, R. B. "Natural Frequencies of Rectangular Plates Using Characteristic Orthogonal Polynomials in Rayleigh-Ritz Method", *Journal of Sound and Vibration*, vol. 102, no. 4, pp. 493-499, 1985

© 2024 by the author(s). Licensee NIJOTECH.
This article is open access under the CC BY-NC-ND license.
http://creativecommons.org/licenses/by-nc-nd/4.0/